

Computational Investigation of Microreactor Configurations for Hydrogen Production from Formic Acid Decomposition Using a Pd/C Catalyst

Hafeez, Sanaa; Al-Salem, Sultan M.; Bansode, Atul; Villa, Alberto; Dimitratos, Nikolaos; Manos, George; Constantinou, Achilleas

DOI

[10.1021/acs.iecr.1c04128](https://doi.org/10.1021/acs.iecr.1c04128)

Publication date

2022

Document Version

Final published version

Published in

Industrial and Engineering Chemistry Research

Citation (APA)

Hafeez, S., Al-Salem, S. M., Bansode, A., Villa, A., Dimitratos, N., Manos, G., & Constantinou, A. (2022). Computational Investigation of Microreactor Configurations for Hydrogen Production from Formic Acid Decomposition Using a Pd/C Catalyst. *Industrial and Engineering Chemistry Research*, 61(4), 1655-1665. <https://doi.org/10.1021/acs.iecr.1c04128>

Important note

To cite this publication, please use the final published version (if applicable). Please check the document version above.

Copyright

Other than for strictly personal use, it is not permitted to download, forward or distribute the text or part of it, without the consent of the author(s) and/or copyright holder(s), unless the work is under an open content license such as Creative Commons.

Takedown policy

Please contact us and provide details if you believe this document breaches copyrights. We will remove access to the work immediately and investigate your claim.

Green Open Access added to TU Delft Institutional Repository

'You share, we take care!' - Taverne project

<https://www.openaccess.nl/en/you-share-we-take-care>

Otherwise as indicated in the copyright section: the publisher is the copyright holder of this work and the author uses the Dutch legislation to make this work public.

Computational Investigation of Microreactor Configurations for Hydrogen Production from Formic Acid Decomposition Using a Pd/C Catalyst

Sanaa Hafeez, Sultan M. Al-Salem, Atul Bansode, Alberto Villa, Nikolaos Dimitratos, George Manos,* and Achilleas Constantinou*



Cite This: *Ind. Eng. Chem. Res.* 2022, 61, 1655–1665



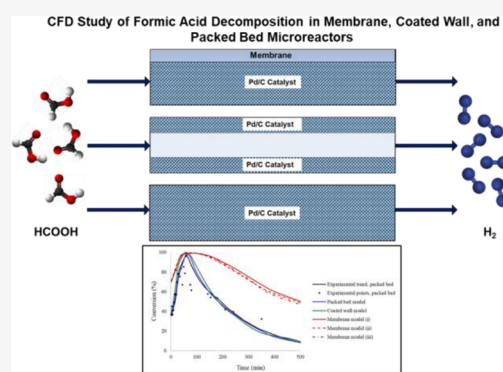
Read Online

ACCESS |

Metrics & More

Article Recommendations

ABSTRACT: The need to replace fossil fuels with sustainable alternatives has been a critical issue in recent years. Hydrogen fuel is a promising alternative to fossil fuels because of its wide availability and high energy density. For the very first time, novel microreactor configurations for the formic acid decomposition have been studied using computational modeling methodologies. The decomposition of formic acid using a commercial 5 wt % Pd/C catalyst, under mild conditions, has been assessed in packed bed, coated wall, and membrane microreactors. Computational fluid dynamics (CFD) was utilized to develop the comprehensive heterogeneous microreactor models. The CFD modeling study begins with the development of a packed bed microreactor to validate the experimental work, subsequently followed by the theoretical development of novel microreactor configurations to perform further studies. Previous work using CFD modeling had predicted that the deactivation of the Pd/C catalyst was due to the production of the poisoning species CO during the reaction. The novel membrane microreactor facilitates the continuous removal of CO during the reaction, therefore prolonging the lifetime of the catalyst and enhancing the formic acid conversion by approximately 40% when compared to the other microreactor configurations. For all microreactors studied, the formic acid conversion increases as the temperature increases, and the liquid flow rate decreases. Further studies revealed that all microreactor configurations had negligible internal and external pore diffusion resistances. The detailed models developed in this work have provided an interesting insight into the intensification of the formic acid decomposition reaction over a Pd/C catalyst.



1. INTRODUCTION

Hydrogen fuel, as an alternative to existing conventional fuels, is environmentally desirable. Some of the features that make hydrogen a promising alternative are a high energy density per mass and a byproduct of water after combustion. Nonetheless, hydrogen suffers from a low energy per unit volume, thus limiting its extensive implementation due to its large volume.¹ On the other hand, formic acid (HCOOH) has attracted great attention in recent years as a promising alternative because it possesses a large quantity of hydrogen (4.3 wt %) and lower toxicities and is widely produced as a product from biomass refinery.^{2–6} In addition, the decomposition of formic acid can offer a continuous production of hydrogen, for fuel cell applications, and has the properties of liquid under standard conditions allowing an instant incorporation into the existing liquid infrastructure.⁷ The production of hydrogen via the formic acid decomposition has prompted research into the application of various catalysts, such as metal oxides,^{8–11} metal carbides,^{1,12–15} and metals, such as Pd and Pt.^{16–25}

Batch reactors have typically been employed to investigate the decomposition of formic acid.^{26–29} Xu et al.²⁰ studied the decomposition of formic acid in a batch reactor using Pd-based catalysts. The Pd/ γ -Al₂O₃ catalyst is susceptible to loss in activity because of the production of the poisonous species CO. It was found that deactivation can be inhibited by the addition of small amounts of oxygen. Furthermore, applying 0.1 vol % of oxygen increases the amount of hydrogen produced as well as prolonging the lifetime of the catalyst. Further increasing the concentration of oxygen enhances the conversion of formic acid but diminishes the yield of hydrogen substantially. Although batch reactors have commonly been

Received: October 17, 2021

Revised: January 10, 2022

Accepted: January 10, 2022

Published: January 20, 2022



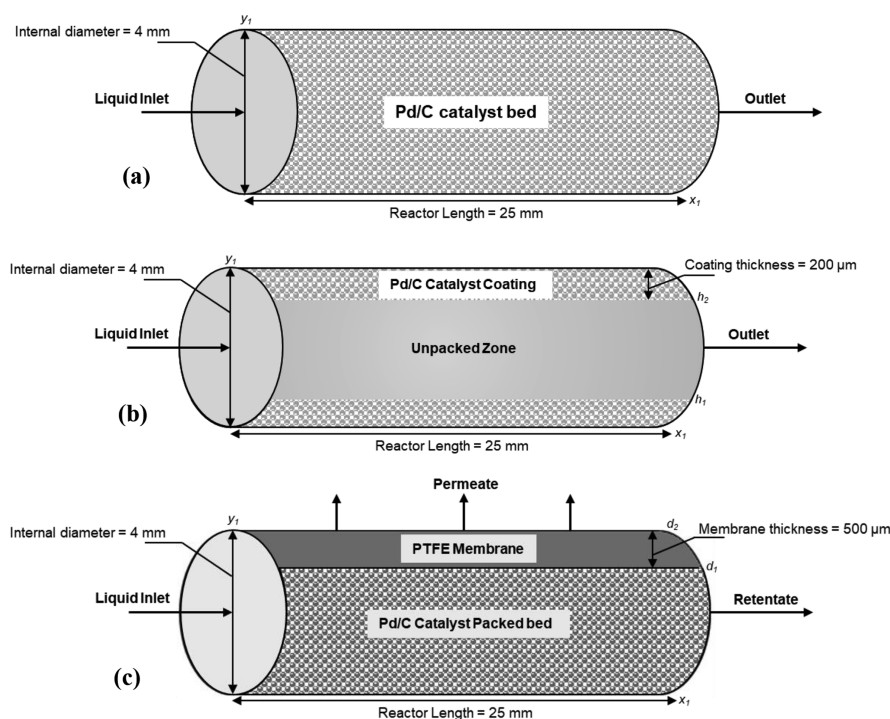


Figure 1. Representation of the (a) fixed bed, (b) coated wall, and (c) membrane microreactors developed for the CFD modeling study.

employed to investigate the decomposition of formic acid, this type of reactor is not able to generate a continuous product output of hydrogen, mainly the application of fuel cell processes. Furthermore, it is often difficult to assess the lifetime of the catalyst in detail to provide an indication of its performance.³⁰

Continuous stirred tank reactors (CSTRs) offer the continuous production of hydrogen for fuel cell applications. Caiti et al.³¹ assessed the performance of batch and CSTR reactors for the formic acid decomposition using a Pd/C catalyst. It was observed that, during continuous operation (plug flow mode), the loss in activity of the Pd/C catalyst is because of poisoning and pore fouling of the formate ions. However, optimistic results can be obtained by performing the formic acid decomposition reaction in a CSTR. As a result, a negligible decrease in catalytic activity for greater than 2500 turnovers is attained under mild conditions. It is highly desirable to investigate other types of continuous flow reactors, such as coated wall and fixed bed reactors for the decomposition of formic acid.

Alternative fuel processes have implemented microreactors. This is because of their superior performance when compared to conventional reactors.³² Membrane reactors have also been utilized to intensify various renewable fuel production reactions. This type of reactor offers several advantages when compared to conventional reactors, such as combining the removal and reaction units into a separate unit.^{33,34} This neglects the requirement for supplementary separation units, enabling the process to become more environmentally sustainable. In addition, membrane reactors increase the selectivities and conversion of reactions, diminish mass transfer resistances, and improve heat transfer.³⁵ Typically, experimental studies are performed to investigate the formic acid decomposition. However, computational modeling techniques have recently been employed using computational fluid

dynamics (CFD) and process flowsheet simulation software to investigate the reaction in detail.^{30,36}

The predominant products from the decomposition of formic acid are hydrogen and CO_2 . The continuous removal of hydrogen during the process could help to alleviate the global issues related to climate change. Membrane separation processes provide a promising outlook to enhance the current process. Current research has shown that a superior purity of hydrogen is attainable by implementing dense metallic membranes, such as Pd, which are selective to hydrogen.³⁷ Furthermore, polymeric and ionic liquid membranes have demonstrated large permeability and selectivity to separate CO from hydrogen.^{38,39}

In this work, the investigation of novel reactor configurations to produce hydrogen from formic acid decomposition, using a 5 wt % Pd/C catalyst, has been studied using CFD. The current study is a continuation of our previous work that displayed a combination of experimental and CFD methodologies to depict the formic acid decomposition, using the same catalyst, in a fixed bed microreactor.³⁰ It was found that the catalyst was susceptible to deactivation in this reactor, and this was attributed to the poisoning species CO. The current work aims to mitigate these effects by developing novel reactor configurations, such as the coated wall and membrane microreactors, to improve the stability of the catalyst. These reformers have not been examined before for this reaction, highlighting the uniqueness and novelty of the current work. For model validation and comparative purposes, the results obtained for the packed bed microreactor³⁰ have been shown in the current work.

Computational analysis using CFD is valuable as it delivers comprehensive details regarding various reaction parameters, such as flows, concentrations, and temperatures. The CFD modeling of packed bed, coated wall, and membrane microreactors has been explored, and their performances are compared and evaluated. A validation of the experimental work

and the modeling work has been conducted, and additional parametric studies, such as internal and external mass transfer limitations, temperature, and flow rates, have been presented.

2. MODELING METHODOLOGY

The experimental work was previously performed using a stainless-steel packed bed microreactor and a commercial 5 wt % Pd/C catalyst for this specific reaction. The temperature of the reactor was maintained between 30 and 60 °C, and an inlet flow rate of 0.05 mL/min formic acid was pumped into the reactor. The Pd/C catalyst was packed into the reactor using glass wool. The particle size ranged from 2 to 6 nm for the fresh Pd/C catalyst and 3 to 15 nm for the utilized catalyst. The mean particle size of Pd nanoparticles expanded from 3.3 ± 0.3 to 4.9 ± 0.3 nm for the old catalyst. A CFD model based upon this experimental work was created, and a good validation with the experimental results was attained. Full specifics of the work upon which the computational modeling study is founded upon can be observed in our previous report.³⁰

In this study, CFD was implemented to establish the heterogeneous particle-fluid transport behavior within the different microreactors. The finite element methodology was used within the CFD modeling procedure. Experimental work is regularly expensive and time consuming when compared to CFD modeling that can effortlessly produce detailed results concerning the space–time variations in the fluid component concentrations, temperatures, and flows. As a result, CFD is a beneficial tool in obtaining reaction/reactor parameters, hence allowing a comprehensive study of the chemical and physical processes involved. This CFD study aims to provide the basis of experimental work to enhance the formic acid decomposition reaction to produce hydrogen in microreactors.

The packed bed, coated wall, and membrane microreactors (Figure 1) were modeled as 2D configurations with the hypotheses that the flow, temperature, and mass profiles appear in the x and y dimensions solely. A previous work has shown that there are negligible differences in the results obtained with either 2D or 3D configurations in microreactors;⁴⁰ therefore, 2D configurations have been adapted for this study. The assumptions that the microreactor models are based upon are as follows: (i) unsteady-state and laminar flow are applicable; (ii) Henry's law is applicable for the membrane–liquid interface; (iii) the microreactors operate isothermally; (iv) insignificant dissolution of liquid in the pervaporation to the gas phase and membrane; (v) the fluid velocity in the axial dimension is continuous with constant transport coefficients and physical properties. The membrane material is polytetrafluoroethylene (PTFE) to facilitate the separation of the gases. Three different membrane configurations were adopted for the CFD modeling: (i) the membrane is solely selective to the removal of CO; (ii) the membrane is selective to the separation of syngas (CO, H₂, and CO₂); (iii) the membrane is selective to the removal of syngas and H₂O. The catalyst used is 5 wt % Pd/C as solid spherical catalyst pellets, and deionized water is utilized as the reaction solvent.

2.1. Reaction Kinetics. The formic acid decomposition can occur from two potential pathways varying based on the reactant conditions and the catalyst used. The first pathway represents formic acid dehydrogenation and generates H₂ and CO₂. The second pathway depicts the formic acid dehydration producing CO and H₂O. The reactions are as follows:



The Pd/C catalyst used for this study has exhibited a 99.9% selectivity toward H₂. In addition, the catalyst possesses a good catalytic activity, TOF = 1136 h⁻¹, under the current reaction conditions in relation to the formic acid dehydrogenation to the products H₂ and CO₂.²⁸ The reaction rate, centered on the formic acid dehydrogenation, is given by

$$r = k \times C^n \quad (3)$$

where r is the rate of reaction, k is the rate constant, C is the concentration of the reacting species, and n is reaction order.²⁸

At lower reaction temperatures of 30 °C, a small amount of CO, approximately 6 ppm, is produced.^{28,30,35} The comprehensive CFD model can be utilized to predict the catalyst activity based on the concentration of CO accumulated during the reaction since poisoning of the catalyst by CO could be a reason to explain the deactivation of the catalyst. At the point of deactivation, the decrease in conversion observed after 75 min is modeled based on the CO concentration (C_{CO}) produced and the activity parameter ($a(t)$)

$$a(t) = 1 - \lambda \times C_{\text{CO}} \quad (4)$$

2.2. Conservation Equations. The conservation equation given for the reacting fluids in the fixed catalyst bed is

$$u_x \frac{\delta c_i}{\delta x} = D_{i,A} \frac{\delta^2 c_i}{\delta x^2} + D_{i,T} \frac{\delta^2 c_i}{\delta y^2} - J_i S_b \quad (5)$$

where u (m/s) is the velocity of the fluid in the axial direction, J_i (mol/m²·s) is the molar flux of the fluid components in the packed bed, and D_i (m²/s) represents the diffusion coefficients in the transverse or axial directions. S represents the surface area of the catalyst particles subjected to the reacting fluids in the catalytic bed and is depicted as

$$S = S_a(1 - \varepsilon) \quad (6)$$

where ε is the porosity of the catalytic bed and S_a (m) is the exterior area of the catalyst pellets. For solid spherical particles, this is expressed as

$$S_a = \frac{3}{r_{pe}} \quad (7)$$

where r_{pe} (m) is the radius of the catalyst particle.

The molar flux is the rate determined by considering the mass balance and the particle-fluid boundary conditions. This can be displayed based upon the external mass transfer coefficient

$$J_i = h_i(c_i - c_{i,ps}) \quad (8)$$

$$h_i = \frac{Sh \cdot D_i}{2r_{pe}} \quad (9)$$

$$Sc = \frac{\mu}{\rho_M \cdot D_i} \quad (10)$$

$$Re = \frac{2r_{pe} \cdot \rho \cdot u_x}{\mu} \quad (11)$$

$$Sh = 2 + 0.552Re^{1/2}Sc^{1/3} \quad (12)$$

where h_i (m/s) is the coefficient representing the external mass transfer, $c_{i,ps}$ (mol/m³) is the chemical species concentration at the exterior of the catalyst particle, and D_i (m²/s) is the molecular diffusion coefficient in the bulk liquid. The dimensionless parameters, Sh , Sc , and Re , represent the Sherwood number, Schmidt number, and Reynolds number, respectively, based upon the Frössling⁴¹ correlation and are related to the transfer of mass occurring at the pellet–fluid interface. μ (Pa·s) and ρ (kg/m³) are the viscosity and density of the fluids, respectively.

The mass balance for the species in the unpacked zone is determined by coupling the reaction domain with the liquid domain. This equation can be expressed as

$$u_x \frac{\delta c_i}{\delta x} = D_i \left(\frac{\delta^2 c_i}{\delta x^2} + \frac{\delta^2 c_i}{\delta y^2} \right) \quad (13)$$

The heterogeneous reaction takes occurring inside the catalyst particles are combined with the conservation equations and COMSOL's reactive pellet bed feature. The conservation equation across the pellet surface at r_{dim} and a predefined additional dimension (1D) on the standardized radius of the catalyst pellet particle ($r = r_{dim}/r_{pe}$) are expressed as

$$\frac{\delta}{\delta r} \left(r^2 D_{i,eff} \frac{\delta c_{i,p}}{\delta r} \right) = r^2 r_{pe} R_{i,p} \quad (14)$$

where $D_{i,eff}$ represents chemical species' effective diffusivity in the pellet pores and $R_{i,p}$ is the reaction source term (rate of reaction/volume of the catalyst particle).

The bulk molecular diffusion coefficient of the reactant in the fluid phase was obtained using the Reddy–Doraiswamy correlation⁴²

$$D_i = 1 \times 10^{-16} \left(\frac{T \sqrt{M_i}}{\mu V_i^{2/3}} \right) \quad (15)$$

where T (K) is the temperature, M_i (g/mol) is the molecular weight of the fluid, and V_i (m³/kmol) is the molar volume at standard boiling conditions. The effective diffusivities of the fluids into the catalyst particle are obtained by describing the diffusion coefficient to the Knudsen or bulk diffusivity

$$D_{i,eff} = \frac{D_i \Phi_p \sigma_c}{\tau} \quad (16)$$

where Φ_p , σ_c , and τ are the pellet porosity, constriction factor, and tortuosity, respectively. Typical values of these are $\sigma_c = 0.8$, $\tau = 3.0$, and $\Phi_p = 0.4$.⁴³

The conservation equation depicting the transport of fluids in the membrane is expressed as

$$D_{i,m} \left(\frac{\delta^2 c_{i,m}}{\delta x^2} + \frac{\delta^2 c_{i,m}}{\delta y^2} \right) = 0 \quad (17)$$

where $c_{i,m}$ is the concentration of the fluids in the membrane and $D_{i,m}$ is the species diffusion coefficient in the membrane.

The fluid dynamics of the microreactor have been modeled using the Navier–Stokes equation. The equations depicting the mass and momentum balances are given by

$$\frac{\partial \rho}{\partial t} + \nabla \cdot (\rho u) = 0 \quad (18)$$

$$\rho \frac{\partial u}{\partial t} + \rho (u \cdot \nabla) u = \nabla \cdot [-PI + \tau] + F \quad (19)$$

where P is the pressure (Pa), τ is the viscous stress tensor (Pa), and F is the volume force vector (N/m³).

The boundary conditions of the packed bed, coated wall, and membrane microreactors are given per the following:

packed bed microreactor

$$\text{at } x = 0; c_i = c_{i,in}, u_y = 0, u_x = u_{in}, \frac{\delta^2 P}{\delta x^2} \quad (20)$$

$$\text{at } x = x_j; \frac{\delta c_i}{\delta x} = 0, u_y = 0, \frac{\delta u_x}{\delta x} = 0, P = P_{out} \quad (21)$$

$$\text{at } y = 0; c_i = 0, u_r = 0, \frac{\delta u_x}{\delta y} = 0, \frac{\delta P}{\delta y} \quad (22)$$

$$\text{at } r = 1; c_{i,p} = c_{i,ps} \quad (23)$$

$$\text{at } r = 0; \frac{\delta c_{i,p}}{\delta r} = 0 \quad (24)$$

coated wall microreactor

$$\text{at } x = 0; c_i = c_{i,in}, u_y = 0, u_x = u_{in}, \frac{\delta^2 P}{\delta x^2} = 0 \quad (25)$$

$$\text{at } x = x_j; \frac{\delta c_i}{\delta x} = 0, u_y = 0, \frac{\delta u_x}{\delta x} = 0, P = P_{out} \quad (26)$$

$$\text{at } y = 0; c_i = 0, u_r = 0, \frac{\delta u_x}{\delta y} = 0, \frac{\delta P}{\delta y} = 0 \quad (27)$$

$$\text{at } r = 1; c_{i,p} = c_{i,ps} \quad (28)$$

$$\text{at } r = 0; \frac{\delta c_{i,p}}{\delta r} = 0 \quad (29)$$

$$\text{at } y = h_1; c_{i,b} = K \times c_i \quad (30)$$

$$\text{at } y = h_2; c_{i,s} = K \times c_i \quad (31)$$

membrane microreactor

$$\text{at } x = 0; c_i = c_{i,in}, u_y = 0, u_x = u_{in}, \frac{\delta^2 P}{\delta x^2} = 0 \quad (32)$$

$$\text{at } x = x_j; \frac{\delta c_i}{\delta x} = 0, u_y = 0, \frac{\delta u_x}{\delta x} = 0, P = P_{out} \quad (33)$$

$$\text{at } y = 0; c_i = 0, u_r = 0, \frac{\delta u_x}{\delta y} = 0, \frac{\delta P}{\delta y} = 0 \quad (34)$$

$$\text{at } r = 1; c_{i,p} = c_{i,ps} \quad (35)$$

$$\text{at } r = 0; \frac{\delta c_{i,p}}{\delta r} = 0 \quad (36)$$

$$\text{at } y = d_1; c_{i,m} = Hc_i \quad (37)$$

$$\text{at } y = d_2; c_{i,m} = c_{i,g} \quad (38)$$

The modeling methodology coupled with the relative conservation and mass balance equations, along with the conditions at the boundary, has been simulated using

COMSOL Multiphysics software version 5.3. A mesh sensitivity study was conducted to investigate the effects of sizing of the mesh on the correctness of the computed theoretical result. Table 1 displays the results from the grid

Table 1. Mesh Sensitivity Analysis Investigation for the Different Microreactor Configurations Used in This Study

packed bed microreactor			
no. of elements	406,118	812,236	1,218,354
X_{HCOOH}	0.0912	0.0911	0.0931
coated wall microreactor			
no. of elements	758,324	1,519,148	2,276,572
X_{HCOOH}	0.0896	0.0896	0.0912
membrane microreactor			
no. of elements	648,527	1,298,704	1,946,981
X_{HCOOH}	0.4852	0.4853	0.4881

sensitivity study utilized for the CFD modeling study. The study was performed at a reaction temperature of 30 °C, pressure of 1 bar, and inlet flow of 0.05 mL/min. The catalyst used is the 0.1 g catalyst of 5 wt % Pd on carbon. The influence of the mesh size was obtained by comparing the reactor outlet conversion of formic acid. It can be observed that, for the coated wall, packed bed, and membrane reactors, grid numbers of 758,324, 406,118, and 648,527 were observed to have the least variation among the studied numbers, respectively. Therefore, the finalized geometry for the packed bed microreactor model consisted of a mesh containing 406,118 domain elements and 2320 boundary elements, with 94,364 degrees of freedom and a computational time of 40 s. The coated wall microreactor model geometry consisted of a mesh containing 758,324 elements, 6587 boundary elements with 101,215 degrees of freedom, and a computational time of 184 s. The membrane microreactor model geometry consisted of a mesh containing 648,527 elements, 5264 boundary elements with 98,897 degrees of freedom, and a computational time of 117 s. The results from all microreactor models were observed to be mesh-independent. A comprehensive list of the CFD modeling parameters utilized for this study can be found in a previously published work.³⁰

3. RESULTS AND DISCUSSION

3.1. Model Validation. The results generated from the CFD modeling studies were compared to the experimental data to establish their validity for the formic acid decomposition. Figure 2 depicts the results obtained for the comparative study among the packed bed, coated wall, and membrane microreactors and the experimental work²⁸ under constant reaction conditions. The membrane microreactor allows the continuous removal of CO during the reaction. The different membrane configurations developed for the CFD modeling were as follows: (i) the membrane is solely selective to the removal of CO; (ii) the membrane is selective to the separation of syngas (CO, H₂, and CO₂); (iii) the membrane is selective to the removal of syngas and H₂O. It can be noted that the formic acid conversion increases with time up to a maximum conversion observed at approximately 75 min, subsequently followed by a decrease in conversion and continues to do so steadily. This decrease in conversion can be attributed to the loss of activity of the Pd/C catalyst. The uncertainty of the modeling results was determined by performing a sensitivity analysis using the diffusion coefficients of the fluids in the microreactors. It was found that, by varying the diffusivity from 1×10^{-9} to 9×10^{-9} m²/s, the modeling results showed that there was a less than 3% discrepancy between the data, confirming the accuracy of the model.

From Figure 2, it can be observed that the CFD modeling results obtained with the coated wall and packed bed microreactors demonstrate a sound validation with the experimental results. The similar operation of these specific reactors is due to the relatively small-scale size of the reactors. Consequently, any mass or heat transfer resistances that may arise between the different microreactors is eliminated, resulting in negligible differences between the formic acid conversions observed for the coated wall and packed bed. However, the coated wall microreactor requires a lower mass of catalyst to achieve similar results with the packed bed microreactor. Therefore, the coated wall microreactor has a superior performance to the packed bed microreactor in terms of smaller amounts of catalyst required to facilitate the production of hydrogen from formic acid decomposition.

The membrane microreactor reveals a further superior performance in terms of the formic acid conversion when compared to the experimental data and the other config-

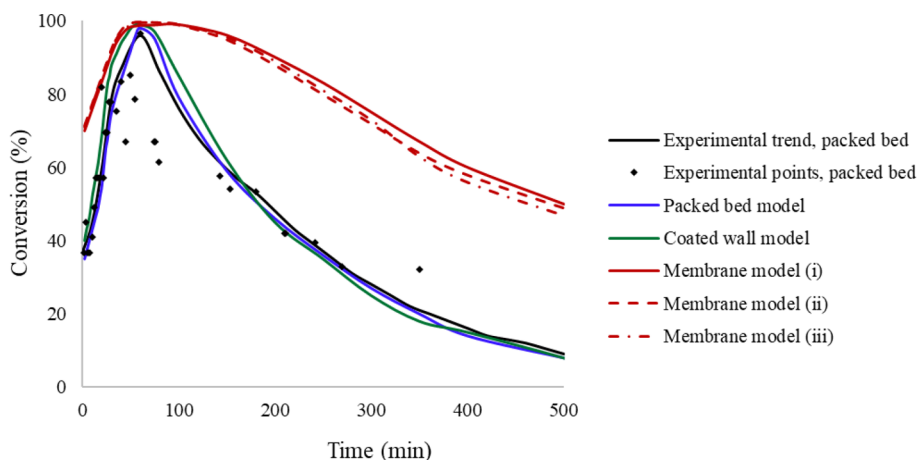


Figure 2. Experimental and CFD modeling results representing the conversion of formic acid against reaction time. Study performed at an inlet flow of 0.05 mL/min, reaction temperature of 30 °C, pressure of 1 bar, and the Pd/C catalyst.

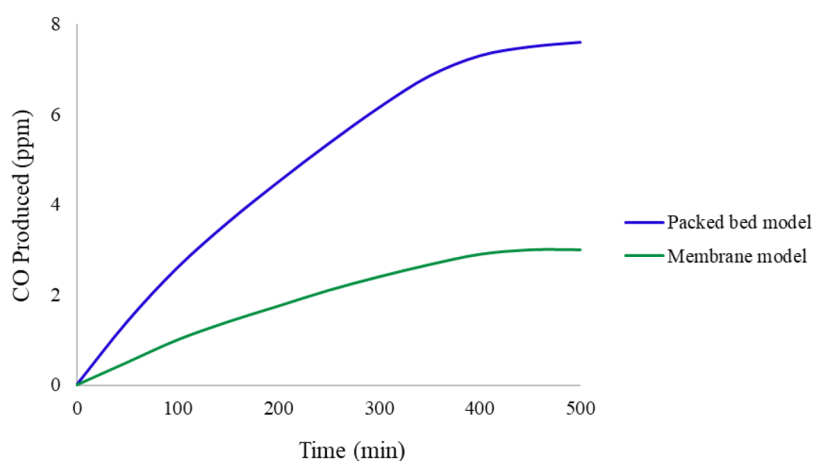


Figure 3. CO generated during reaction for the packed bed and membrane microreactors. Study performed at an inlet flow of 0.05 mL/min, reaction temperature of 30 °C, pressure of 1 bar, and the Pd/C catalyst.

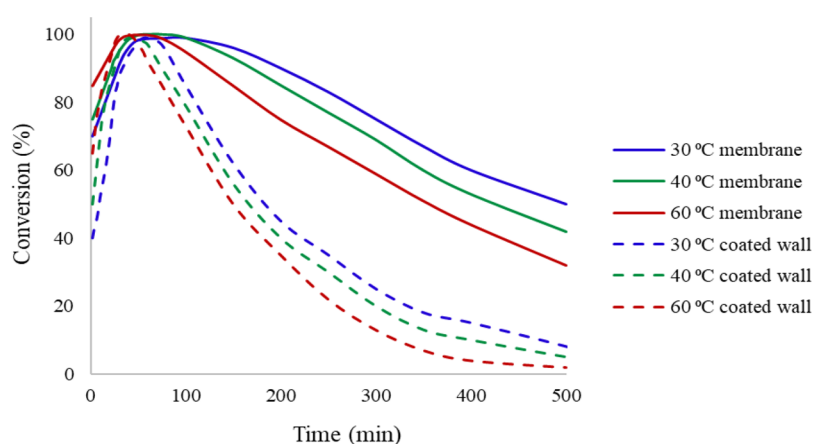


Figure 4. Impacts of temperature on the formic acid conversion using coated wall and membrane microreactors. Study performed at an inlet flow of 0.05 mL/min, reaction temperature of 30 °C, pressure of 1 bar, and the Pd/C catalyst.

urations. From Figure 2, it can be noted that the conversion of the membrane reactor at 500 min is approximately 40% greater than the conversions achieved by the coated wall and packed bed microreactors. Furthermore, at longer reaction times greater than 500 min, the conversion of formic acid appears to reach a plateau, as opposed to the other configurations, which reveal the conversion of formic acid to continuously decrease. The deactivation of the Pd/C catalyst has been previously modeled using CFD and proved that the decrease in catalytic activity is due to the poisoning species CO.³⁰ At milder reaction temperatures of 30 °C, a relatively small amount of CO is produced (6 ppm).²⁸ The detailed heterogeneous models can be implemented to predict the catalytic activity relative to the amount of CO produced during the reaction.

Figure 3 displays the amount of CO produced with respect to time in the fixed bed and membrane microreactors. It can be noticed that the amount of CO generated in the membrane microreactor is significantly lower than that produced in the packed bed microreactor. The lower concentration of CO present in the membrane microreactor results in the higher conversion of formic acid observed in Figure 2. This is because CO poisons the Pd/C catalyst leading to lower conversions with time for the formic acid decomposition reaction. The activity of the Pd/C catalyst can be decreased by strong chemisorption of reaction products or intermediates, such as CO and H₂O, and the increment of the mean particle size.^{31,44}

The production of the poisonous species CO can explain the loss in conversion of formic acid. The membrane microreactor models enable the continuous removal of CO from the reacting fluids. As a result, the Pd/C catalyst retains a higher catalytic activity over a constant period, hence prolonging the lifetime of the catalyst. The different membrane microreactor configurations have demonstrated a similar performance, confirming the idea that the deactivation of the Pd/C catalyst is related to the concentration of CO.

3.2. Effects of Temperature and Liquid Flow Rate.

The effects of temperature on the formic acid conversion were investigated for the coated wall and membrane microreactors. Full details of the parametric studies performed for the packed bed microreactor can be found in a previous work.³⁰ Figure 4 displays how the conversion of formic acid varies with temperature. The temperatures investigated were 30, 40, and 60 °C, with all other reaction conditions kept constant. High temperatures are not typically studied for the decomposition of formic acid as portable devices that implement formic acid fuel cells necessitate milder reaction conditions. Increasing the temperature results in an increase in the formic acid conversion for both microreactor configurations. This behavior is expected according to the Arrhenius expression, $k = Ae^{-E_a/RT}$, which generates an activation energy of 39 kJ/mol for the formic acid decomposition using a Pd/C catalyst. Furthermore, it can be observed that the undesired pathway is thermodynamically

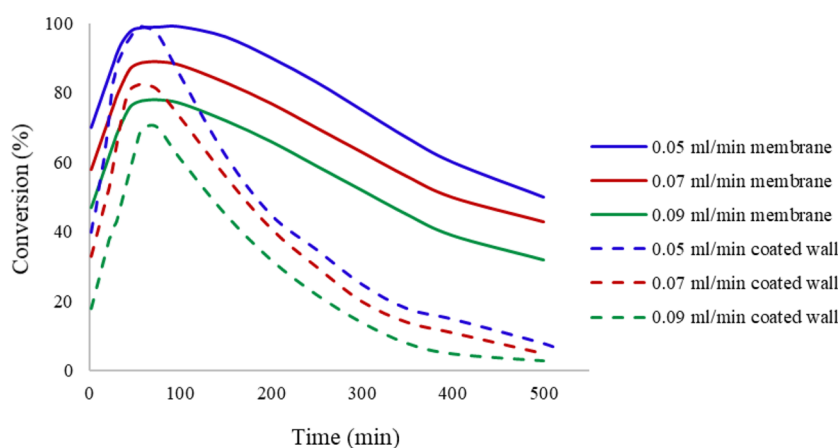


Figure 5. Formic acid inlet liquid flow against the formic acid conversion using coated wall and membrane microreactors. Study performed at a reaction temperature of 30 °C, pressure of 1 bar, and the Pd/C catalyst.

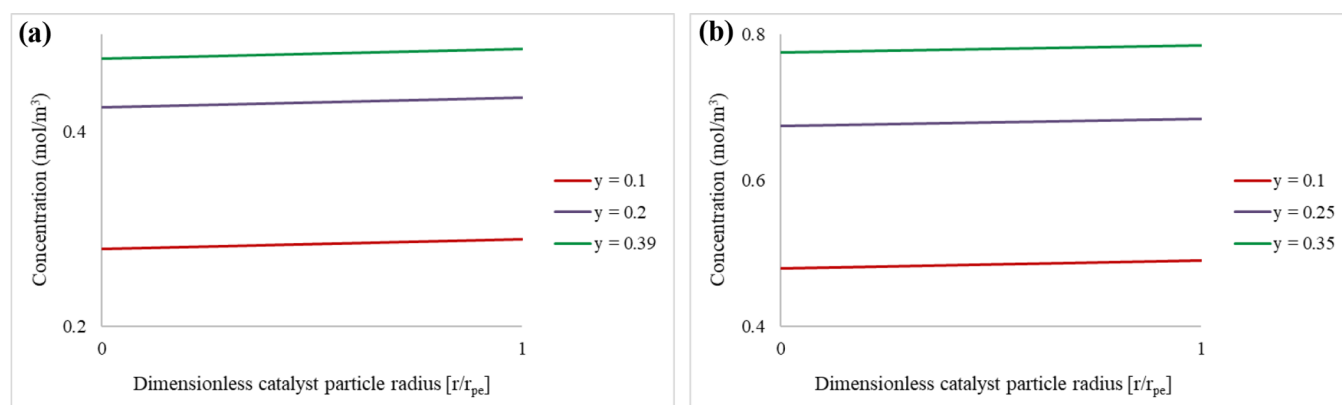


Figure 6. Formic acid concentration profiles within the catalyst particles at $x = 1.25$ cm for the (a) coated wall microreactor and (b) membrane microreactor. Study performed at an inlet flow of 0.05 mL/min, reaction temperature of 30 °C, pressure of 1 bar, and the Pd/C catalyst.

avored at higher temperatures, indicating the promotion of the dehydration pathway and facilitating the production of the poisonous species CO.

Caiti et al.³¹ studied the formic acid dehydrogenation for continuous hydrogen production using a Pd/C catalyst. The effects of temperature on the formic acid conversion were studied in a plug flow reactor (PFR) using a temperature range of 30–110 °C. It was observed that increasing the reaction temperature led to an increase in the activity of the Pd/C catalyst, with the turnover frequency of the catalyst increasing from 1500 h⁻¹ at 50 °C to 5860 h⁻¹ at 110 °C. Furthermore, an increase in the rate of deactivation (k_d) is also observed with increasing temperatures, implying a temperature dependence on the catalytic deactivation. The results from this study agree with the results depicted in the current work.

The inlet liquid flow rate of formic acid was investigated on the conversion of formic acid for the coated wall and membrane microreactors. The inlet liquid flow rates varied from 0.05 to 0.09 mL/min, and all other reaction conditions were constantly maintained. It can be observed in Figure 5 that increasing the liquid flow rate results in the decrease in the formic acid conversion. This is true for both the coated wall and membrane microreactors. When an experimental liquid flow rate of 0.05 mL/min was used, the conversion of formic acid initially increases and then decreases (Figure 2). Increasing the liquid flow rate produces lower formic acid conversions. This is the expected result as the flow rate

increases the reacting species using a smaller amount of time within the microreactors, leading to a decrease in the conversion of formic acid. These results agree with the dependence of conversion of formic acid with the space velocity.

3.3. Internal and External Mass Transfer Resistances.

In a multiphase chemical reaction with catalyst pellets, the mass transfer of reactants will initially occur from the bulk fluid to the outer surface of the catalyst pellet. Subsequently, the reacting fluids diffuse from the outer catalytic surface into and through the pores of the catalyst pellet, with the reaction solely occurring on the catalytic surface of the pores. The CFD models can be used to predict the pore diffusion limitations occurring within the reactor and enable a greater understanding of whether the reaction is diffusion-limited or rate-limited. The internal mass transfer resistances were studied by comparing the concentration profiles at the center of the catalyst pellet ($r = 0$) to $r = 1$. The pore diffusion limitations were investigated by using a reactor axial length of $x = 1.25$ cm and varying radial heights (mm) for the coated wall and membrane microreactors. Figure 6 displays the variation of the concentration within the catalyst pellet for the coated wall and membrane microreactors. From the results, it can be determined that there are negligible differences in the concentrations observed from the exterior of the catalyst particle to the center of the particle. Similar results were observed for the fixed bed microreactor.³⁰ Therefore, there are

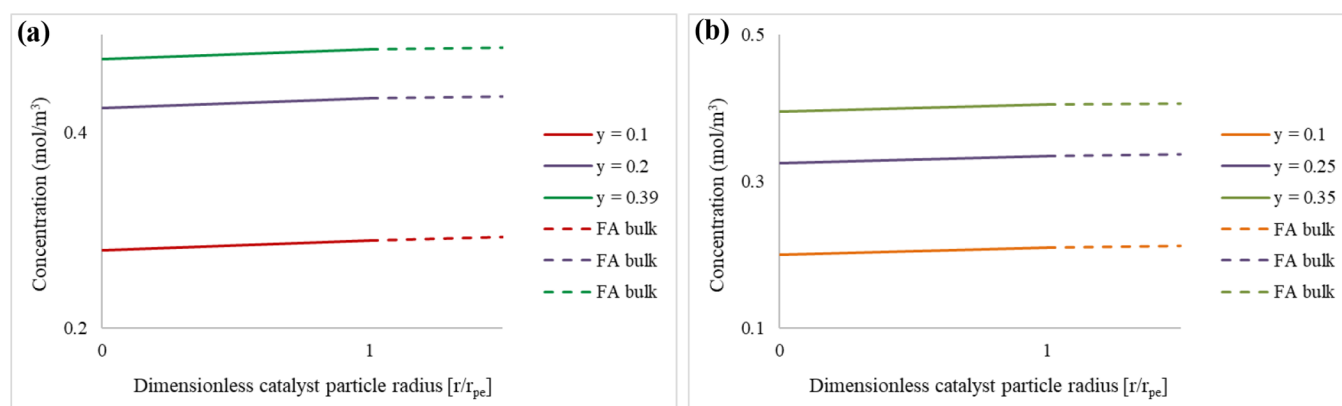


Figure 7. Formic acid concentration profiles within the catalyst particles and in the bulk fluid at $x = 1.25$ cm using (a) coated wall and (b) membrane microreactors. Study performed at an inlet flow of 0.05 mL/min, reaction temperature of 30 °C, pressure of 1 bar, and the Pd/C catalyst.

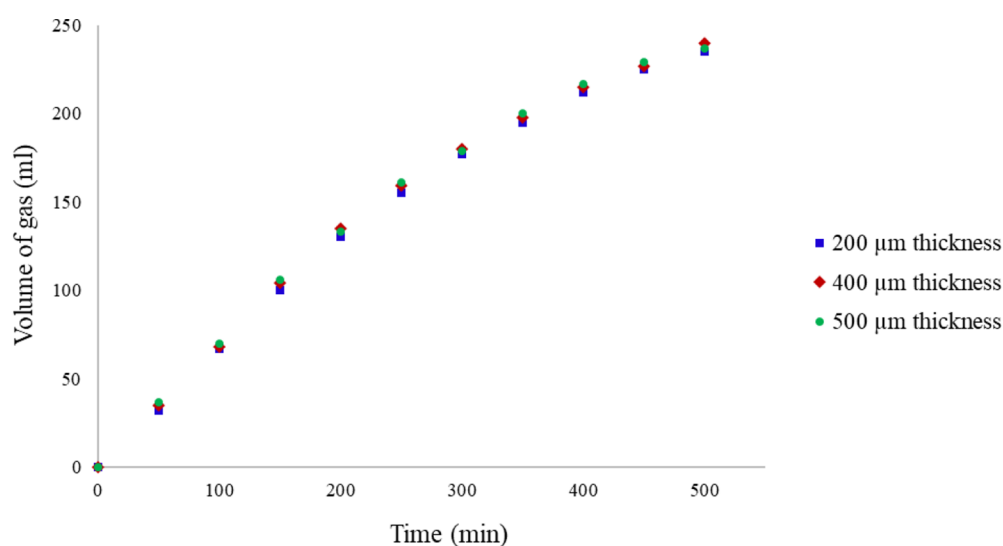


Figure 8. Influence of catalyst coating thickness on the volume of gas generated, with respect to time, in the coated wall microreactor. Study performed at an inlet flow of 0.05 mL/min, reaction temperature of 30 °C, pressure of 1 bar, and the Pd/C catalyst.

insignificant internal mass transfer limitations for the reactors used in this study; hence, the reaction is surface reaction-limited.

The external mass transfer limitations were studied by evaluating the concentrations of the bulk reacting fluid with the concentrations at the outer shell of the catalyst particle. The developed rigorous two-phase models incorporate the dimensionless parameters depicted in eqs 8–12. These models incorporate the dimensionless numbers (Schmidt, Sherwood, and Reynolds) to predict directly the mass transfer aspects. Figure 7 displays the concentration profiles observed in the microreactors. There are insignificant variations in conversion between the exterior of the catalyst pellet and the bulk reacting fluid. Therefore, there are negligible external mass transfer resistances for the microreactors developed in this study. The packed bed microreactor also displayed similar results.³⁰ Figure 8 displays the effects of catalyst coating thickness on the volume of gas generated during the formic acid decomposition. The mass of the catalyst was maintained at a constant value by adjusting the porosity of the catalyst coating in the coated wall reformer. The results show that varying the catalyst coating thickness has negligible impacts on the formic acid conversion; therefore, minimal effects on the volume of gas were produced.

These results confirm the preceding conclusion that, within the microreactor, there were insignificant mass transfer resistances.

3.4. Effect of Membrane Thickness and Catalyst Coating Thickness. The membrane thickness effect was studied using the membrane microreactor model, and the results are observed in Figure 9. There is less than 5% discrepancy in the formic acid conversion when varying the thickness of the membrane from 0.1 to 0.9 mm. Furthermore, there is no significant effect observed on the deactivation of the Pd/C catalyst. These findings imply that the transfer resistance of the gases in the membrane has negligible effects on the performance of the microreactor due to the high permeability of the PTFE membrane. The diffusion coefficients of the produced gases based on the concentrations in the liquid phase were obtained by relating the diffusion coefficient of the gases in the membrane ($D'_{i,m}$) based on the concentration of the gases in the gas phase with the dimensionless Henry solubility (H) of the produced gases in the liquid

$$D'_{i,m} = D_{i,m} \times H \quad (39)$$

The variation of the thickness of the catalyst in the coated wall reformer is important in determining the performance of the microreactor. Increasing the thickness of the catalyst

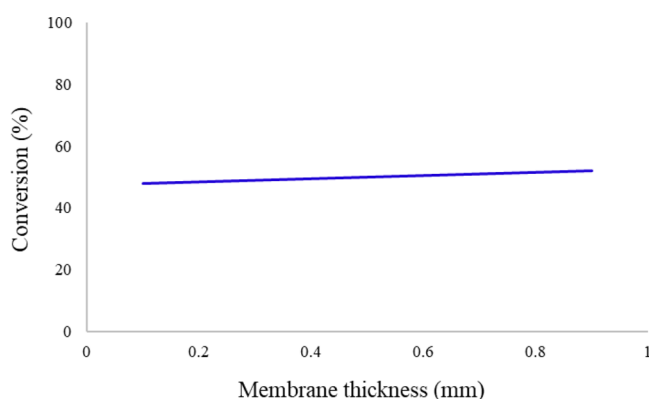


Figure 9. Influence of membrane thickness on the formic acid conversion. Study performed at an inlet flow of 0.05 mL/min, reaction temperature of 30 °C, pressure of 1 bar, and the Pd/C catalyst.

coating will lead to higher reaction rates, which will enhance the conversion of formic acid, and subsequently the production of hydrogen. The dimensionless parameter e signifies the fraction of the coating thickness of the catalyst to the width of the microreactor. A packed bed reactor would depict a ratio of $e = 1$. From Figure 10, it can be noted that, as the thickness of

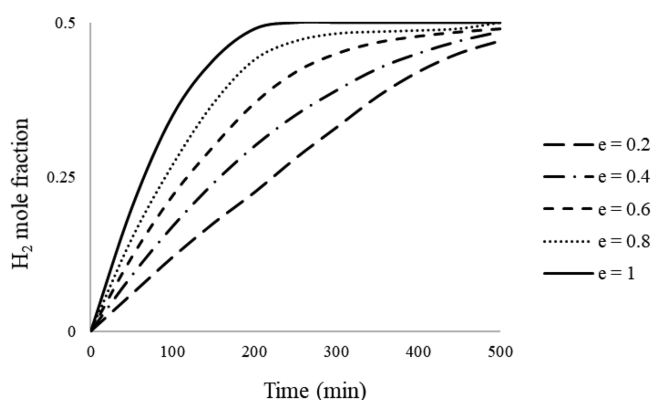


Figure 10. Mole fraction of hydrogen produced with time for varying catalyst coating thicknesses in the coated wall microreactor. Study performed at an inlet flow of 0.05 mL/min, reaction temperature of 30 °C, pressure of 1 bar, and the Pd/C catalyst.

the catalyst coating increases, the conversion of formic acid is enhanced, resulting in a higher production of hydrogen. Furthermore, when $e \sim 0.6$, the production of hydrogen reaches a maximum, indicating a maximum conversion of formic acid. Increasing the ratio any further results in a higher production rate of hydrogen. Therefore, the value of e should be maintained at approximately 0.6 and above to promote the highest production rates of hydrogen.

4. CONCLUSIONS

Novel microreactor configurations for the formic acid decomposition, using a 5 wt % Pd/C catalyst, have been investigated using CFD modeling. Computational methods were employed to investigate the formic acid decomposition in novel microreactor configurations over 5 wt % Pd/C. The results show that the coated wall and packed bed microreactors exhibited a comparable performance with each other as well as the experimental data. However, the coated wall microreactor

requires a lower mass of the catalyst as opposed to the packed bed microreactor, suggesting the superiority of the coated wall configuration. On the other hand, the membrane microreactor model displayed a significantly enhanced performance when compared to the other microreactors. Previous work using CFD modeling had suggested that the loss of catalytic activity of the Pd/C catalyst, in the packed bed microreactor, was due to the production of the poisonous species CO. The membrane microreactor facilitates the continuous removal of CO during the reaction, thus prolonging the activity of the Pd/C catalyst. As a result, the conversion of formic acid is enhanced, and the production of hydrogen increases. Although the commercial Pd/C catalyst suffers from deactivation using the commonly studied packed bed and batch reactors, this work has proven that the effects of deactivation can be alleviated using a membrane microreactor. This configuration can potentially make the decomposition of formic acid more suitable for practical applications.

Furthermore, it was found that, in the case of all microreactors, increasing the temperature led to higher conversions of formic acid; however, this also promoted the deactivation of the catalyst. This suggests that the deactivation of the solid Pd/C catalyst is temperature-dependent. Further investigations revealed that there are insignificant internal and external mass transfer limitations for all microreactor configurations. Increasing the thickness of the membrane was observed to have insignificant effects on the conversion of formic acid owing to the high permeability of the membrane. Enhanced formic acid conversion was discovered when the catalyst coating thickness was increased in a coated wall microreactor. The detailed CFD models designed in this study have provided some interesting and innovative insights into the formic acid decomposition reaction. The superior performances of the coated wall and membrane microreactor models have offered a practical basis for experimental work to implement these novel reactors for the current reaction. Future research could be directed toward implementing these microreactors on an experimental scale and prolonging the activity of the solid catalysts by minimizing the accumulation of CO.

AUTHOR INFORMATION

Corresponding Authors

George Manos – Department of Chemical Engineering, University College London, London WC1E 7JE, UK; Email: g.manos@ucl.ac.uk

Achilleas Constantinou – Department of Chemical Engineering, Cyprus University of Technology, 3036 Limassol, Cyprus; orcid.org/0000-0002-7763-9481; Email: a.konstantinou@cut.ac.cy

Authors

Sanaa Hafeez – Department of Chemical Engineering, University College London, London WC1E 7JE, UK

Sultan M. Al-Salem – Environment & Life Sciences Research Centre, Kuwait Institute for Scientific Research, Safat 13109, Kuwait; orcid.org/0000-0003-0652-4502

Atul Bansode – Catalysis Engineering, Department of Chemical Engineering, Delft University of Technology, 2629 HZ Delft, Netherlands

Alberto Villa – Dipartimento di Chimica, Università degli Studi di Milano, 20133 Milan, Italy; orcid.org/0000-0001-8656-6256

Nikolaos Dimitratos – Dipartimento di Chimica Industriale e dei Materiali, ALMA MATER STUDIUM Università di Bologna, 40136 Bologna, Italy

Complete contact information is available at:
<https://pubs.acs.org/10.1021/acs.iecr.1c04128>

Author Contributions

The manuscript was written through contributions of all authors. All authors have given approval to the final version of the manuscript.

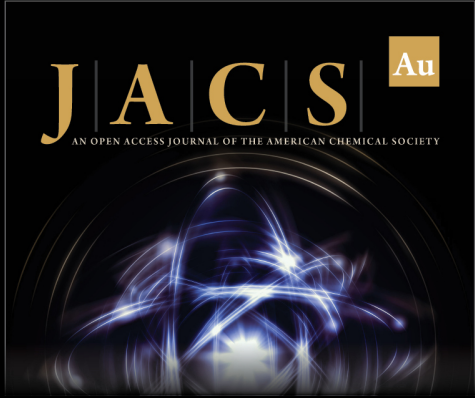
Notes

The authors declare no competing financial interest.

REFERENCES


- (1) Carrales-Alvarado, D.; Dongil, A.; Fernández-Morales, J.; Fernández-García, M.; Guerrero-Ruiz, A.; Rodríguez-Ramos, I. Selective hydrogen production from formic acid decomposition over Mo carbides supported on carbon materials. *Catal. Sci. Technol.* **2020**, *10*, 6790–6799.
- (2) Baena-Moreno, F. M.; Pastor-Perez, L.; Zhang, Z.; Reina, T. Stepping towards a low-carbon economy. Formic acid from biogas as case of study. *Appl. Energy* **2020**, *268*, 115033.
- (3) Chen, X.; Liu, Y.; Wu, J. Sustainable production of formic acid from biomass and carbon dioxide. *Mol. Catal.* **2020**, *483*, 110716.
- (4) Hou, Y.; Niu, M.; Wu, W. Catalytic oxidation of biomass to formic acid using O₂ as an oxidant. *Ind. Eng. Chem. Res.* **2020**, *59*, 16899–16910.
- (5) Valentini, F.; Kozell, V.; Petrucci, C.; Marrocchi, A.; Gu, Y.; Gelman, D.; Vaccaro, L. Formic acid, a biomass-derived source of energy and hydrogen for biomass upgrading. *Energy Environ. Sci.* **2019**, *12*, 2646–2664.
- (6) Voß, D.; Pickel, H.; Albert, J. Improving the fractionated catalytic oxidation of lignocellulosic biomass to formic acid and cellulose by using design of experiments. *ACS Sustainable Chem. Eng.* **2019**, *7*, 9754–9762.
- (7) Bhandari, S.; Rangarajan, S.; Maravelias, C. T.; Dumesic, J. A.; Mavrikakis, M. Reaction mechanism of vapor-phase formic acid decomposition over platinum catalysts: DFT, reaction kinetics experiments, and microkinetic modeling. *ACS Catal.* **2020**, *10*, 4112–4126.
- (8) Zacharska, M.; Chuvilin, A. L.; Kriventsov, V. V.; Beloshapkin, S.; Estrada, M.; Simakov, A.; Bulushev, D. A. Support effect for nanosized Au catalysts in hydrogen production from formic acid decomposition. *Catal. Sci. Technol.* **2016**, *6*, 6853–6860.
- (9) Ai, M. Activities for the decomposition of formic acid and the acid-base properties of metal oxide catalysts. *J. Catal.* **1977**, *50*, 291–300.
- (10) Onishi, H.; Aruga, T.; Iwasawa, Y. Catalytic reactions on a metal oxide single crystal: Switchover of the reaction paths in formic acid decomposition on titanium dioxide TiO₂ (110). *J. Am. Chem. Soc.* **1993**, *115*, 10460–10461.
- (11) Trillo, J.; Munuera, G.; Criado, J. Catalytic decomposition of formic acid on metal oxides. *Catal. Rev.* **1972**, *7*, 51–86.
- (12) Gray, J. T.; Kang, S. W.; Yang, J.-I.; Kruse, N.; McEwen, J.-S.; Park, J. C.; Ha, S. Unravelling the reaction mechanism of gas-phase formic acid decomposition on highly dispersed Mo₂C nanoparticles supported on graphene flakes. *Appl. Catal., B* **2020**, *264*, 118478.
- (13) Agrawal, K.; Roldan, A.; Kishore, N.; Logsdail, A. J. Dehydrogenation and dehydration of formic acid over orthorhombic molybdenum carbide. *Catal. Today* **2021**, *384*, 197–208.
- (14) Kurnia, I.; Yoshida, A.; Situmorang, Y. A.; Kasai, Y.; Abudula, A.; Guan, G. Utilization of dealkaline lignin as a source of sodium-promoted MoS₂/Mo₂C hybrid catalysts for hydrogen production from formic acid. *ACS Sustainable Chem. Eng.* **2019**, *7*, 8670–8677.
- (15) Cao, J.; Wang, J.; Ma, Y.; Li, X.; Xiaokaiti, P.; Hao, X.; Abudula, A.; Guan, G. Hydrogen production from formic acid over morphology-controllable molybdenum carbide catalysts. *J. Alloys Compd.* **2018**, *735*, 1463–1471.
- (16) Alshammari, H. M.; Alotaibi, M. H.; Aldosari, O. F.; Alsolami, A. S.; Alotaibi, N. A.; Alzahrani, Y. A.; Alhumaimess, M. S.; Alotaibi, R. L.; El-Hiti, G. A. A Process for Hydrogen Production from the Catalytic Decomposition of Formic Acid over Iridium–Palladium Nanoparticles. *Materials* **2021**, *14*, 3258.
- (17) Barlocco, I.; Bellomi, S.; Delgado, J. J.; Chen, X.; Prati, L.; Dimitratos, N.; Roldan, A.; Villa, A. Enhancing activity, selectivity and stability of palladium catalysts in formic acid decomposition: Effect of support functionalization. *Catal. Today* **2021**, *382*, 61–70.
- (18) Li, F.; Xue, Q.; Ma, G.; Li, S.; Hu, M.; Yao, H.; Wang, X.; Chen, Y. Formic acid decomposition-inhibited intermetallic Pd₃Sn₂ nanonetworks for efficient formic acid electrooxidation. *J. Power Sources* **2020**, *450*, 227615.
- (19) Sanchez, F.; Bocelli, L.; Motta, D.; Villa, A.; Albonetti, S.; Dimitratos, N. Preformed Pd-Based Nanoparticles for the Liquid Phase Decomposition of Formic Acid: Effect of Stabiliser, Support and Au–Pd Ratio. *Appl. Sci.* **2020**, *10*, 1752.
- (20) Xu, P.; Bernal-Juan, F. D.; Lefferts, L. Effect of oxygen on formic acid decomposition over Pd catalyst. *J. Catal.* **2021**, *394*, 342–352.
- (21) Kim, Y.; Kim, S.-H.; Ham, H. C.; Kim, D. H. Mechanistic insights on aqueous formic acid dehydrogenation over Pd/C catalyst for efficient hydrogen production. *J. Catal.* **2020**, *389*, 506–516.
- (22) Kosider, A.; Blaumeiser, D.; Schötz, S.; Preuster, P.; Bösmann, A.; Wasserscheid, P.; Libuda, J.; Bauer, T. Enhancing the feasibility of Pd/C-catalyzed formic acid decomposition for hydrogen generation—catalyst pretreatment, deactivation, and regeneration. *Catal. Sci. Technol.* **2021**, *11*, 4259–4271.
- (23) Santos, J. L.; Megías-Sayago, C.; Ivanova, S.; Centeno, M. Á.; Odriozola, J. A. Functionalized biochars as supports for Pd/C catalysts for efficient hydrogen production from formic acid. *Appl. Catal., B* **2021**, *282*, 119615.
- (24) Sneka-Plątek, O.; Kaźmierczak, K.; Jędrzejczyk, M.; Sautet, P.; Keller, N.; Michel, C.; Ruppert, A. M. Understanding the influence of the composition of the AgPd catalysts on the selective formic acid decomposition and subsequent levulinic acid hydrogenation. *Int. J. Hydrogen Energy* **2020**, *45*, 17339–17353.
- (25) Zhang, J.; Wang, H.; Zhao, Q.; Di, L.; Zhang, X. Facile synthesis of PdAu/C by cold plasma for efficient dehydrogenation of formic acid. *Int. J. Hydrogen Energy* **2020**, *45*, 9624–9634.
- (26) Hu, C.; Pulleri, J. K.; Ting, S.-W.; Chan, K.-Y. Activity of Pd/C for hydrogen generation in aqueous formic acid solution. *Int. J. Hydrogen Energy* **2014**, *39*, 381–390.
- (27) Detwiler, M. D.; Milligan, C. A.; Zemlyanov, D. Y.; Delgass, W. N.; Ribeiro, F. H. Kinetics of gas phase formic acid decomposition on platinum single crystal and polycrystalline surfaces. *Surf. Sci.* **2016**, *648*, 220–226.
- (28) Sanchez, F.; Motta, D.; Roldan, A.; Hammond, C.; Villa, A.; Dimitratos, N. Hydrogen generation from additive-free formic acid decomposition under mild conditions by Pd/C: Experimental and DFT studies. *Top. Catal.* **2018**, *61*, 254–266.
- (29) Sanchez, F.; Alotaibi, M. H.; Motta, D.; Chan-Thaw, C. E.; Rakotomahevitra, A.; Tabanelli, T.; Roldan, A.; Hammond, C.; He, Q.; Davies, T.; Villa, A.; Dimitratos, N. Hydrogen production from formic acid decomposition in the liquid phase using Pd nanoparticles supported on CNFs with different surface properties. *Sustainable Energy Fuels* **2018**, *2*, 2705–2716.
- (30) Hafeez, S.; Sanchez, F.; Al-Salem, S. M.; Villa, A.; Manos, G.; Dimitratos, N.; Constantinou, A. Decomposition of additive-free formic acid using a Pd/C catalyst in flow: Experimental and CFD modelling studies. *Catalysts* **2021**, *11*, 341.
- (31) Caiti, M.; Padovan, D.; Hammond, C. Continuous production of hydrogen from formic acid decomposition over heterogeneous nanoparticle catalysts: from batch to continuous flow. *ACS Catal.* **2019**, *9*, 9188–9198.


- (32) Hafeez, S.; Manos, G.; Al-Salem, S.; Aristodemou, E.; Constantinou, A. Liquid fuel synthesis in microreactors. *React. Chem. Eng.* **2018**, *3*, 414–432.
- (33) Wu, G.; Cao, E.; Ellis, P.; Constantinou, A.; Kuhn, S.; Gavriilidis, A. Continuous flow aerobic oxidation of benzyl alcohol on Ru/Al₂O₃ catalyst in a flat membrane microchannel reactor: An experimental and modelling study. *Chem. Eng. Sci.* **2019**, *201*, 386–396.
- (34) Wu, G.; Cao, E.; Ellis, P.; Constantinou, A.; Kuhn, S.; Gavriilidis, A. Development of a flat membrane microchannel packed-bed reactor for scalable aerobic oxidation of benzyl alcohol in flow. *Chem. Eng. J.* **2019**, *377*, 120086.
- (35) Hafeez, S.; Al-Salem, S.; Manos, G.; Constantinou, A. Fuel production using membrane reactors: a review. *Environ. Chem. Lett.* **2020**, *18*, 1477–1490.
- (36) Hafeez, S.; Barlocco, I.; Al-Salem, S.; Villa, A.; Xiaowei, C.; Delgado, J. J.; Manos, G.; Dimitratos, N.; Constantinou, A. Experimental and Process Modelling Investigation of the Hydrogen Generation from Formic Acid Decomposition Using a Pd/Zn Catalyst. *Appl. Sci.* **2021**.
- (37) Adhikari, S.; Fernando, S. Hydrogen membrane separation techniques. *Ind. Eng. Chem. Res.* **2006**, *45*, 875–881.
- (38) Peer, M.; Mehdi Kamali, S.; Mahdeyarfar, M.; Mohammadi, T. Separation of hydrogen from carbon monoxide using a hollow fiber polyimide membrane: experimental and simulation. *Chem. Eng. Technol.: Industrial Chemistry-Plant Equipment-Process Engineering-Biotechnology* **2007**, *30*, 1418–1425.
- (39) Zarca, G.; Ortiz, I.; Urtiaga, A. Copper (I)-containing supported ionic liquid membranes for carbon monoxide/nitrogen separation. *J. Membr. Sci.* **2013**, *438*, 38–45.
- (40) Hafeez, S.; Aristodemou, E.; Manos, G.; Al-Salem, S.; Constantinou, A. Modelling of packed bed and coated wall microreactors for methanol steam reforming for hydrogen production. *RSC Adv.* **2020**, *10*, 41680–41692.
- (41) Frossling, N. Über die verdunstung fallender tropfen. *Gerlands Beitr. Geophys.* **1938**, *52*, 170–216.
- (42) Reddy, K.; Doraiswamy, L. Estimating liquid diffusivity. *Ind. Eng. Chem. Fundam.* **1967**, *6*, 77–79.
- (43) Fogler, H., *Chapter 15: diffusion and reaction Elements of Chemical Reaction Engineering*. Englewood Cliffs, NJ: Prentice Hall: 2016.
- (44) Bulushev, D. A.; Beloshapkin, S.; Ross, J. R. Hydrogen from formic acid decomposition over Pd and Au catalysts. *Catal. Today* **2010**, *154*, 7–12.



JACS Au
AN OPEN ACCESS JOURNAL OF THE AMERICAN CHEMICAL SOCIETY

Editor-in-Chief
Prof. Christopher W. Jones
Georgia Institute of Technology, USA

Open for Submissions 

pubs.acs.org/jacsau  ACS Publications
Most Trusted. Most Cited. Most Read.